SAND2018-10773C

A demonstration of force estimation and regularization methods for multi-shaker testing

Ryan Schultz
Structural Dynamics Department
Sandia National Laboratories[1]
P.O. box 5800 – MS0557
Albuquerque, NM, 87185
rschult@sandia.gov

Abstract
Design of multiple-input/multiple-output vibration experiments, such as impedance matched multi-axis testing and multi-shaker testing, rely on a force estimation calculation which is typically executed using a direct inverse approach. Force estimation can be performed multiple ways, each method providing some different tradeoff between response accuracy and input forces. Additionally, there are ways to improve the numerics of the problem with regularization techniques which can reduce errors incurred from poor conditioning of the system frequency response matrix. This paper explores several different force estimation methods and compares several regularization approaches using a simple multiple-input/multiple-output dynamic system, demonstrating the effects on the predicted inputs and responses.

Keywords: multiple-input/multiple-output, force estimation, regularization, conditioning

1 Introduction

Multiple-input/multiple output (MIMO) vibration testing is becoming more popular. Techniques such as the impedance-matched multi-axis test (IMMAT) method have shown great promise in using multiple shaker inputs to achieve good matches to response of dynamic systems in complicated environments, such as acoustic environments [1, 2]. These tests rely on MIMO control systems to determine the shaker inputs based on the system frequency response function (FRF) matrix and the target responses, typically in the form of a cross-power spectral density (CPSD) matrix. An input or force estimation method is used to invert that FRF matrix and provide an estimate of the inputs which matches the target responses [3, 4].

Inverting the FRF matrix introduces errors into the estimated inputs if the FRF matrix is poorly conditioned, which is typically the case for most dynamic systems. The condition number typically peaks at modes of the system, where the system response is dominated by a single mode. Numerical corrections, called regularization, can be used to change the FRF matrix to reduce the condition number and reduce the errors in the input estimation [5, 6, 7]. The objective of a good regularization scheme is to change the FRF matrix enough that errors will be small, while not changing it so much that it loses the important dynamics or changes the overall form of the matrix. Here, singular value and Tikhonov regularization methods are demonstrated on a simple MIMO dynamic system, a plate with multiple shaker inputs.

There are multiple force estimation methods, three of which are explored here: the standard direct method, the independent drives method, and the buzz test method [8, 9]. Each method is used to determine shaker inputs to replicate the response of the plate model to an acoustic, distributed pressure environment. The responses are compared at target, or control, locations and reference, or non-control locations in terms of the auto-power spectral density (APSD) as well as coherence and phase between response points.

2 Example Dynamic System and FRFs

For this study, a model-based approach is used because the system FRF can easily be modified to examine the effects of different input or output locations. Here, a free-free 12 inch by 24 inch by ¼ inch aluminum plate is the dynamic system. The

[1] Sandia National Laboratories is a multimission laboratory managed and operated by National Technology and Engineering Solutions of Sandia, LLC., a wholly owned subsidiary of Honeywell International, Inc., for the U.S. Department of Energy's National Nuclear Security Administration under contract DE-NA0003525

finite element (FE) model of the plate uses only out-of-plane displacements, so there are three DOF per node. 40 modes were computed which covers a frequency range up to 2800 Hz, sufficient for the 2000 Hz bandwidth of interest for this study. This bandwidth covers both low and high modal density regions. Modal damping is used with values between 0.2 to 1.0 percent, increasing with mode frequency and FRFs are computed from the modes using a modal FRF calculation.

3 Condition Number of the FRF Matrix

The first study examines how the system inputs, outputs, damping and noise affect the condition number of the FRF matrix. It is widely understood that a "bad" condition number causes errors when doing an inversion of the FRF matrix. The first step is to understand what causes the condition number of the matrix to change. The next step, discussed in the next section, is to understand how a "bad" condition number translates to errors in the predictions when using an inverse of the FRF matrix in a force estimation process.

The condition number of a matrix is simply the ratio of the largest and smallest singular values. Large singular values indicate large, independent contributions to the overall matrix. For example, the singular values of a response matrix can identify the number of intendent sources which caused the response. For a FRF matrix, the singular values roughly indicate the number of contributing modes at a given frequency line. This is shown in the plots below, where an example FRF is shown as a sum of modal contributions. Take for example the region around 800 Hz, where the FRF is dominated by a single mode. Around 800 Hz, the condition number becomes large and there is one large singular value and several small singular values. Between peaks in the FRF, there are several modes which contribute at similar levels and also several singular values of similar levels.

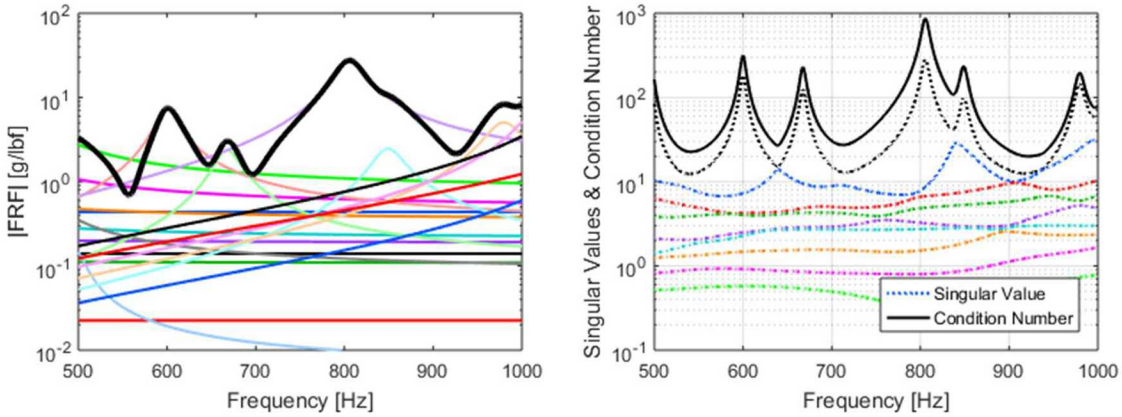

Figure 1: Left: FRF shown as a sum of modal contributions. Right: Singular values (dotted) and condition number (solid).

3.1 Number and Location of Inputs or Outputs

As condition number is a measure of independence of the vectors in a matrix, the input and output locations of a FRF matrix will therefore affect the condition number. For example, if the input or output locations are very similar or tightly-packed, the FRFs for each location will be approximately similar and therefore less independent and the condition number will be large. Conversely, if the input or output locations are chosen to have good independence, then the condition number will be smaller. There are various methods to choose gage locations to achieve good independence, such as methods based on effective independence, condition number minimization or minimizing the off-diagonal terms in the modal assurance criterion (MAC) matrix [10, 11, 12].

To demonstrate how input or output locations affect condition number, two systems were contrived, each with 12 outputs and nine inputs. The "good" system has nine input locations chosen with a condition number minimization method, so the inputs have good independence. The "bad" system has nine input locations chosen very close together, which should make the FRFs for those inputs very similar (i.e. not independent). Input and output locations for these systems are shown below in Figure 2. The condition number computed from the FRF matrices of these two systems is shown in Figure 3. Clearly, the "good" system has a much lower condition number than the "bad" system, by around an order of magnitude over the entire bandwidth.

Next, the number of inputs and outputs was changed for the "good" system to demonstrate how adding or removing gages affects condition number. The gages to add or remove were not chosen using any method, they were simply chosen without analysis. The results, shown in Figure 4, are interesting: removing a gage reduces the condition number, but adding a gage may

increase or decrease the condition number. It is not simply the number of gages which determines the condition number. More important are the locations of the gages and the independence of the entire set of input and output locations.

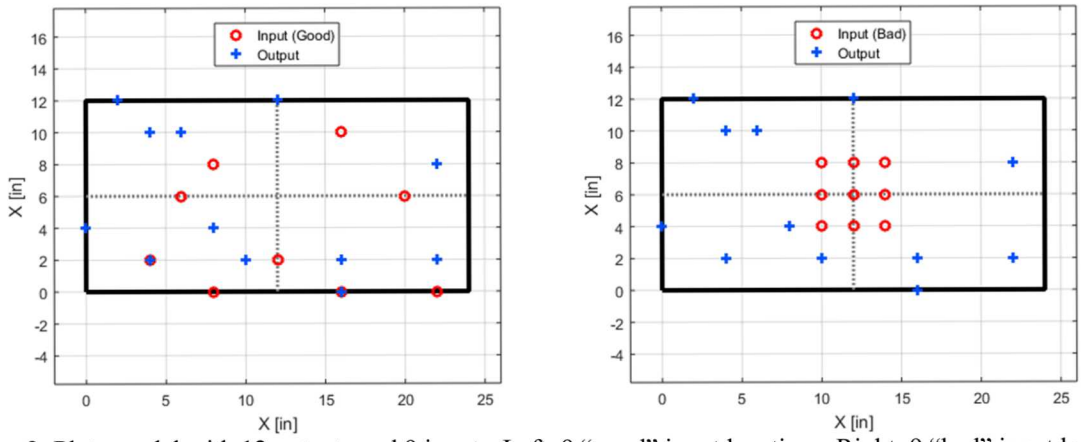

Figure 2: Plate model with 12 outputs and 9 inputs. Left: 9 “good” input locations. Right: 9 “bad” input locations.

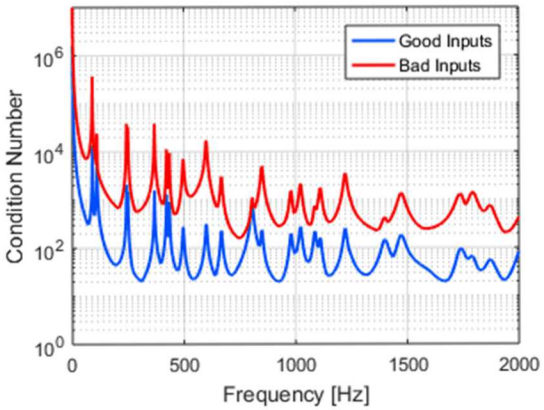

Figure 3: Condition number of FRF matrix with “good” and “bad” input locations

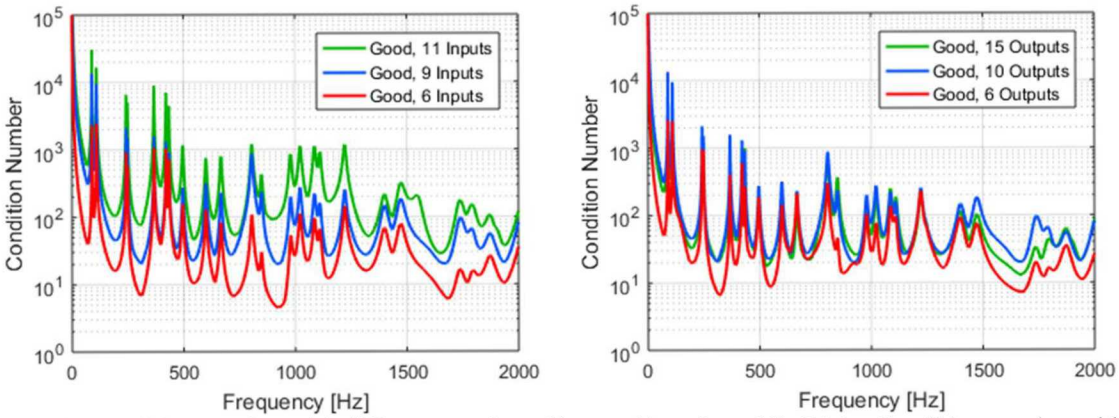

Figure 4: Left: Condition number with different number of inputs (6 vs. 9 vs. 11). Right: Condition number with different number of outputs (6 vs. 10 vs. 15)

3.2 Higher Damping

Next, the damping of the system was increased to observe how damping affects condition number. Here, the modal damping was increased by a factor of four for all modes. Figure 5 shows that increasing damping reduces the condition number at peaks in the FRF. Interestingly, the condition number is not affected between peaks, which is consistent with how damping affects the FRF amplitude.

3.3 Noise on the FRFs

To examine the effects of noise, the FRFs are transformed to impulse responses with an inverse Fourier transform. Then, unique Gaussian noise is added to each impulse response. Finally, the noisy impulse response is transformed back to an FRF with the Fourier transform. This provides noisy FRFs which look like typical test data, where the peaks are cleanly represented but the noise contaminates the valleys and anti-resonances.

Adding noise to the FRFs resulted in approximately the same condition number as the original system, except for the first couple of peaks. So, simply having noise on the FRF estimates does not cause the condition number to increase. In this case, the noise is uncorrelated for each FRF in the matrix. One could imagine if the noise were correlated, as is the case with 60 Hz noise, then the condition number would be increased as the vectors would become non-independent if they are dominated by correlated noise.

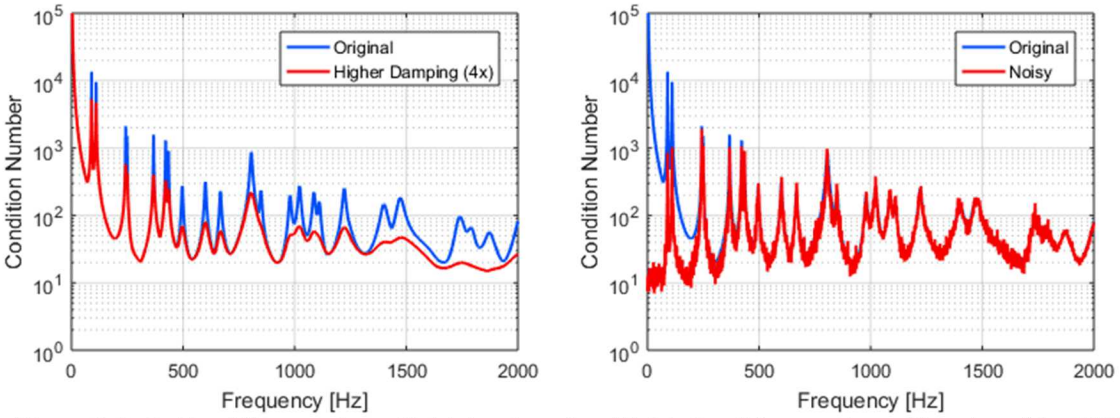

Figure 5: Left: Condition number with higher damping. Right: Condition number with noise of the FRFs

4 Errors Due to Poor Conditioning

Now that the condition number of the FRF matrix has been examined, the next step is to demonstrate how a poor condition number affects results. The general process is to use the measured FRF matrix in a force estimation calculation to estimate the inputs to achieve some desired response of the system. This force estimation generally uses an inverse (or pseudo-inverse) of the FRF matrix. Inverting poorly conditioned matrices causes problems in that noise is propagated or amplified through the poorly-estimated features in the FRF. This is typically shown using perturbation theory where the example system is [13]:

$$Ax = b. \tag{1}$$

Here, A would be the FRF matrix, x would be the input spectra, and b would be the response spectra. If there is noise or uncertainty, e, in the target response spectra, then the system is:

$$Ax = b + e. \tag{2}$$

Estimated inputs from this noisy target response would be:

$$x = A^{+}(b + e), \tag{3}$$

where A^{+} is the pseudo-inverse of the matrix. If A is nicely conditioned, then the response error is not amplified through A^{+} and the effect on the estimated inputs, x, is small. If A is poorly conditioned, the response error is amplified in the estimated inputs. This is explained nicely in [13] and also in [6].

To demonstrate how condition number affects the estimated inputs, a simple example problem was developed using the "good" and "bad" systems described above, each with the higher damping levels (4x). A white noise input was generated to obtain some response, called the "truth" response:

$$S_{aa,0} = HS_{ff,0}H^H = HIH^H \,, \tag{4}$$

where the truth input cross-power spectral density (CPSD) matrix, $S_{ff,0}$, is simply the identity matrix for each frequency line. H^H is the Hermetian (conjugate transpose) of the FRF matrix. The resulting truth response CPSD matrix is $S_{aa,0}$. The objective is to see how slight perturbations (errors or noise) in the truth responses affect the inputs estimated with a direct force estimation calculation, given by:

$$S_{ff,1} = H^+ S_{aa,e} H^{+H}, \tag{5}$$

where $S_{ff,1}$ is the estimated input CPSD and $S_{aa,e}$ is the truth response with some error. Error on the truth response was obtained by Equation 4 with $S_{ff,0}$ having 0.001% random change to the APSDs and 0.001 random change to the coherence and phase. This represents a nearly imperceptible change to the input and resulting response, shown in Figure 6.

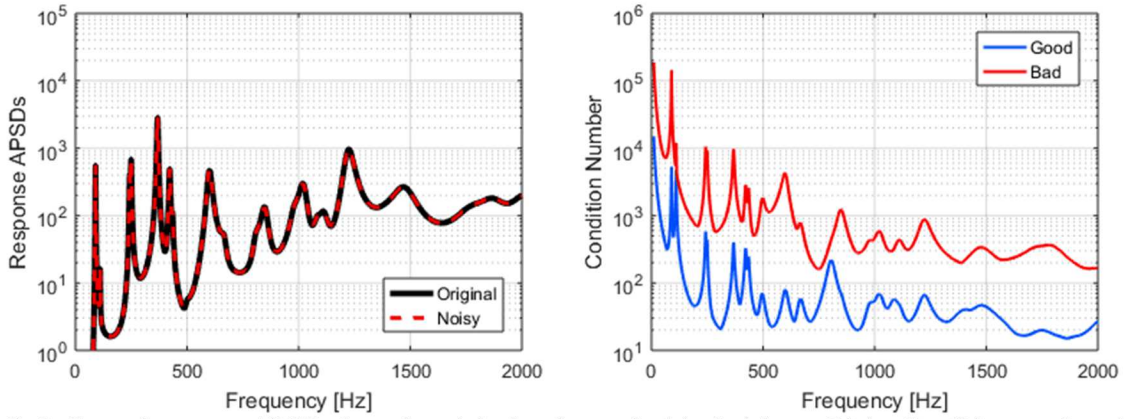

Figure 6: Left: Sum of response APSDs from the original and perturbed (noisy) input. Right: Condition number of the "good" and "bad" inputs configuration for this system

4.1 Example: Sensitivity to Errors in the Input

Figure 7 below shows the dB errors in the estimated responses for nine inputs for the "good" and "bad" systems, represented as an root-mean square (RMS) over the nine inputs. dB error here is computed as the dB error in the input and response APSDs, G_{ff}, G_{aa}:

$$dB_{input} = 10\log_{10}\left(\frac{G_{ff,1}}{G_{ff,0}}\right) \tag{6}$$

$$dB_{response} = 10\log_{10}\left(\frac{G_{aa,1}}{G_{aa,0}}\right) \tag{7}$$

The "bad" system has high error up to approximately 1000 Hz and the "good" system only has errors below approximately 200 Hz. For each system, the errors occur where there are peaks in the condition number, shown in Figure 6. Interestingly, the errors seem to correspond to condition numbers above around 1000. This corresponds to comments in [6] regarding condition number and significant error propagation in generic systems. For each system, there is little error above 1000 Hz; both systems have condition numbers below 1000 above 1000 Hz.

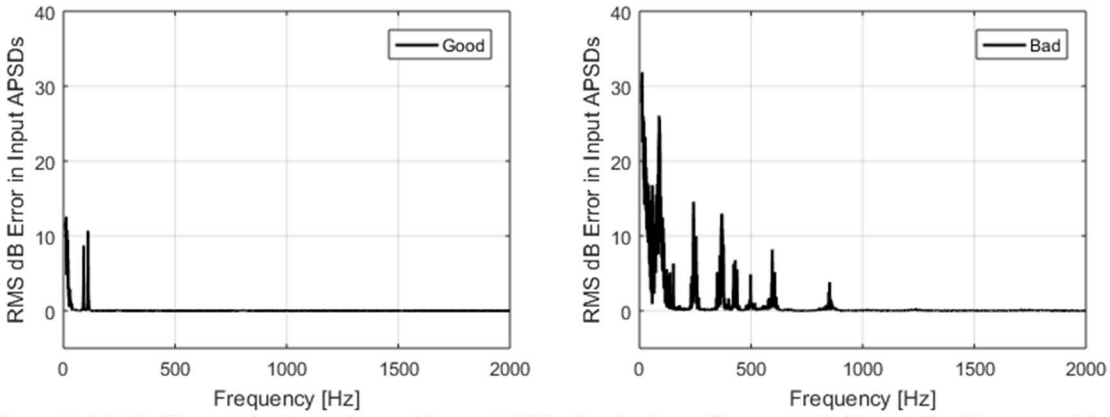

Figure 7: RMS dB error in the estimated input APSDs for the "good" system (left) and "bad" system (right).

The estimated response, $S_{aa,1}$, is computed from the forward equation:

$$S_{aa,1} = HS_{ff,1}H^H. \tag{8}$$

While it is possible that errors in the estimated inputs, $S_{ff,1}$, could cancel out and result in a response with little or no error, this is not generally true. For example, the estimated responses for the "bad" system with a noisy truth response matrix show large errors, Figure 8. Like the estimated inputs, the estimated responses have errors only where the condition number is large.

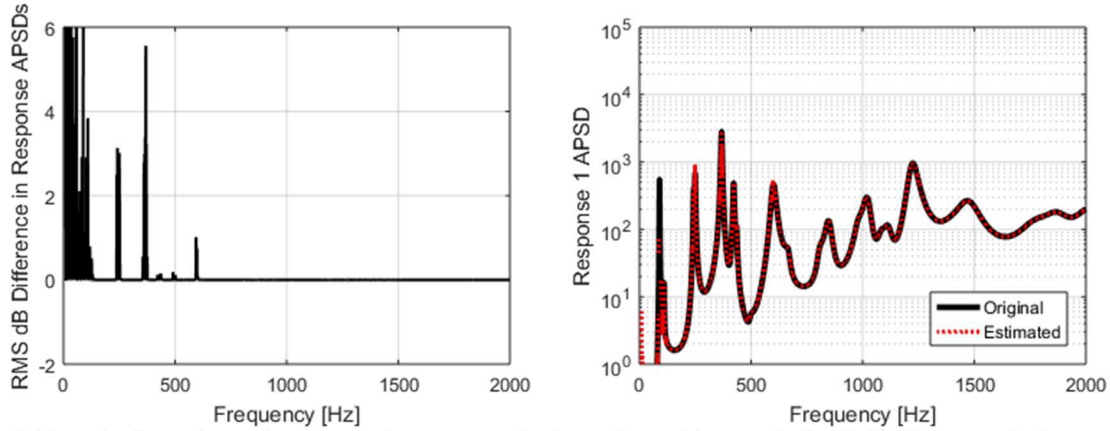

Figure 8: Error in the estimated response due to errors in the estimated inputs. Left: RMS dB error relative to the truth response. Right: APSD at Accel. 1.

5 Numerical Correction - Regularization

Typically, matrices with condition number issues are remedied using some type of regularization. Regularization methods "clean up" small singular values, reducing the condition number and reducing the effects of errors on the estimated inputs. The objective of regularization is to change the FRF matrix enough to reduce the effects of those errors while not changing the overall form. Too much regularization can alter the important information in the matrix, such as the peak amplitudes or phase. The sections below examine different regularization methods and show how they can be used to reduce the error in the estimated inputs.

5.1 Singular Value Truncation and Perturbation

Regularization can be performed by simply modifying the singular values of the FRF matrix. As the condition number is directly tied to the singular values, changing the singular values changes the condition number. The objective is to modify the small singular values to they do not amplify errors. Changing the large singular values would drastically change the form of the matrix, so that is not desirable. Note that for very large matrices, computing the singular value decomposition (SVD) can be prohibitively expensive and it is more desirable to use some other regularization method, such as Tikhonov (discussed in

the next section). However, for modal testing or multi-shaker testing the number of inputs and outputs is small and computing the SVD of the FRF matrix is trivial so using SVD-based regularization is tractable.

Two methods of changing the singular values are demonstrated here. Both compute the singular value decomposition of the FRF matrix at each frequency line. Regularization is obtained by modifying the singular values which are smaller than some threshold value. The FRF matrix is then re-formed with those new singular values, shown notionally in Equation 7, where S' is the matrix of modified singular values:

$$H = USV^H \rightarrow H' = US'V^H \ . \tag{9}$$

The threshold value can be determined by dividing the maximum singular value by some desired condition number. For example, the threshold value for a vector of singular values, s, and a desired condition number of 1000 would be:

$$s_{threshold} = \max(s)\ /1000 \ . \tag{10}$$

The first method is singular value truncation, wherein the singular values below the threshold are simply set to zero, which has the effect of reducing the rank of the matrix. The second method perturbs the small singular values to larger, but still small values. Making the smallest singular values slightly larger improves the condition number and reduces the errors while still preserving the form of the matrix. Obviously, choosing too high a threshold would have a detrimental effect for either method. In the first, a high threshold would result in zeroing out important information in the FRF matrix. In the second method, a high threshold would increase unimportant information to the same order of magnitude as important information, ruining the form of the matrix.

Figure 9 shows the effect of these singular value regularization methods. By truncating small values to zero or setting small values to larger values, the errors at peaks is greatly reduced. Either method works well in general, with the errors reduced at the peaks while not introducing significant errors elsewhere.

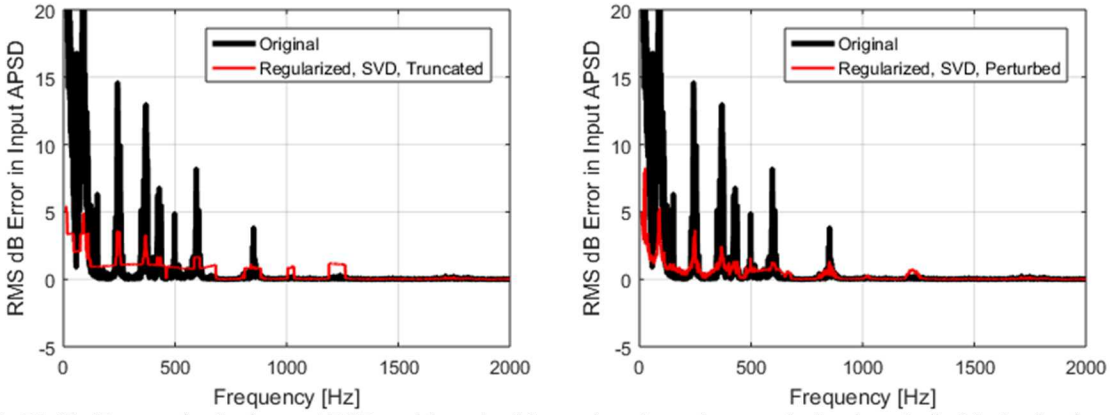

Figure 9: RMS dB error in the input APSDs with and without singular value regularization. Left: Method using truncated singular values. Right: Method using perturbed singular values.

5.2 Tikhonov Regularization

Tikhonov regularization is a very popular regularization method. It has the benefit of not requiring a singular value decomposition. Rather, it simply perturbs the matrix directly in the Moore-Penrose pseudo-inverse. The Moore-Penrose pseudo-inverse of a matrix, A, is given by:

$$A^+ = (A^T A)^{-1} A^T \tag{11}$$

Tikhonov regularization adds a diagonal matrix of regularization parameter values, λ, to the $A^T A$ argument in the inverse, which has the effect of improving the condition number [5]:

$$A^+ = (A^T A + \lambda^2 I)^{-1} A^T \tag{12}$$

For the complex-valued FRF matrices here, this looks like:

$$H'^{+} = (H^H H + \lambda^2 I)^{-1} H^H \tag{13}$$

The regularization value can be a constant – the same value applied to the matrix at all frequency lines, or it can be variable, changing with each frequency line. For a variable value, the value at each frequency line is determined based on the Frobenius norm of the $H^H H$ matrix:

$$\lambda_i^2 = \lambda_o^2 \|H^H H\|_2. \tag{14}$$

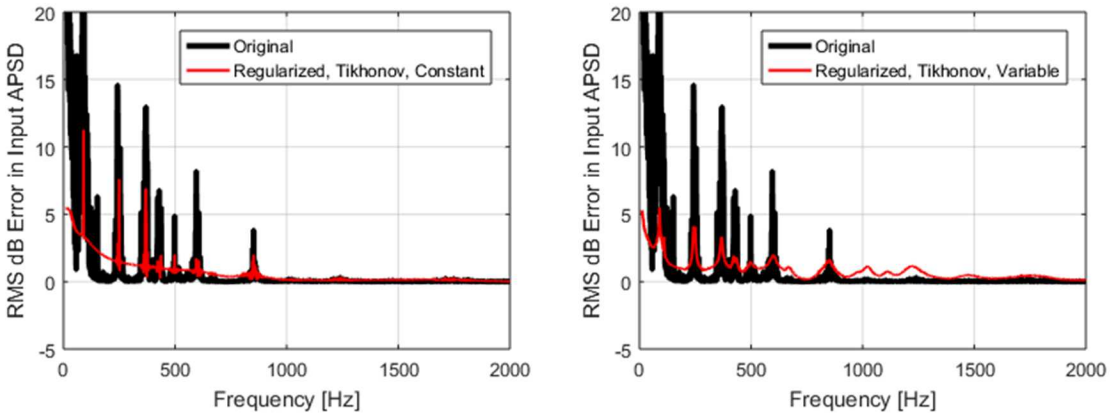

Figure 10: RMS dB error in the input APSDs with and without Tikhonov regularization. Left: Constant regularization parameter value. Right: Variable regularization parameter value.

5.3 Choosing Regularization Parameter Values

It is evident that a regularization value (or singular value threshold) too large would result in a change in the overall form of the matrix. Similarly, too small a value would not sufficiently perturb the system FRF matrix and would not have a regularizing effect. Thus, there is an optimum value. Choosing optimum values is beyond the scope of this paper, but is discussed in the literature, for example in [5]. Instead, a simple demonstration is shown in Figure 11 where the regularization value is changed to be larger or smaller than the nominal value by an order of magnitude. For both singular value and Tikhonov regularization, using too small a value does not result in much error reduction. Interestingly, using too much regularization, while reducing errors at the peaks, introduces new errors elsewhere. This is the result of changing the overall form of the matrix with too large a regularization value. Figure 12 shows the same input APSD error plots but for the "good" system. Again, errors are reduced with proper regularization, and new errors are introduced with too much regularization.

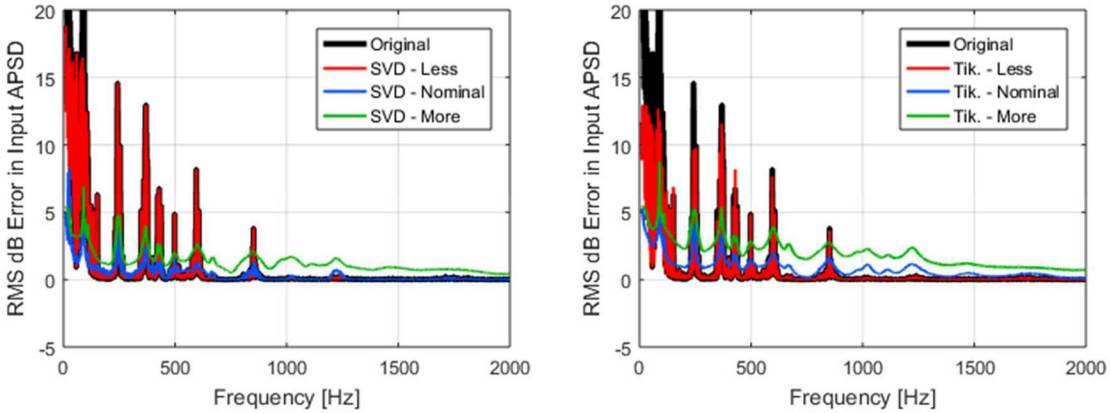

Figure 11: RMS dB error in the inputs, showing the effect of regularization parameter value for SVD (left) and Tikhonov (right) regularization methods

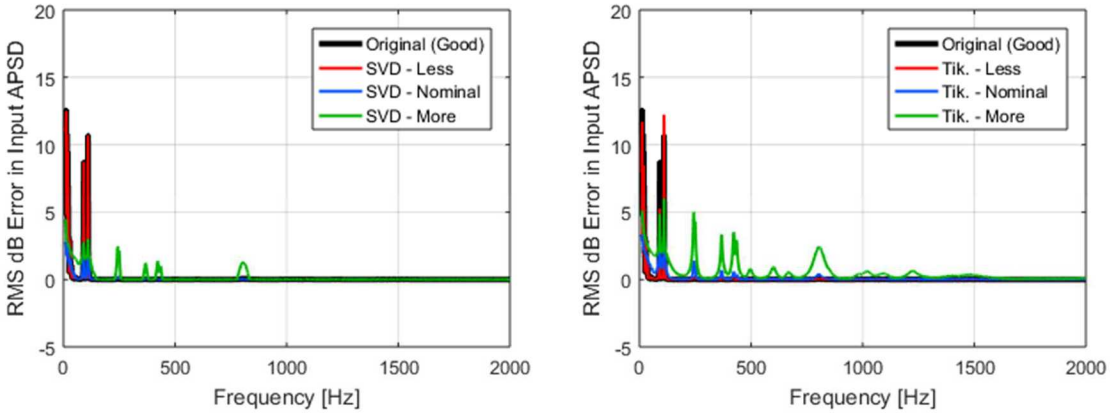

Figure 12: Regularization applied to the "good" system. Left: Singular value regularization. Right: Tikhonov regularization.

6 Force Estimation Methods

In this section, various force estimation methods are compared using the plate model and some acoustic pressure truth environment. The objective here is not to choose one single best method. Rather, it is to show that the force estimation method does matter and each method has specific benefits and faults. The key takeaway is simply that the force estimation method is another tool for the test engineer to use to tailor the test to achieve specific objectives.

The general process is as follows. First, a "truth test" is simulated wherein the plate model is subject to forces over the entire surface representing an acoustic environment. This generates target responses, captured at 12 points. Next, shakers are applied to a just nine input locations and the FRFs between those nine inputs and 12 outputs is computed. This FRF matrix is then used to estimate the inputs which can best match the target responses, using different force estimation methods. Finally, those estimated inputs are used in a "replica test", a forward calculation to estimate the replicated responses and compare those to the target, truth responses. Results for the different force estimation methods are then compared in terms of the inputs and outputs.

6.1 Responses from a Truth Test

Here, the "truth" environment is a set of forces over the entire surface of the plate, which represent acoustic pressures in a diffuse field. These distributed, correlated inputs of the diffuse acoustic field were chosen because it should generate response which cannot completely be replicated by a small number of shaker inputs. Additionally, this is a typical use case for multi-shaker testing – the truth environment is complicated, perhaps acoustic or aero-acoustic. Then, in the lab, the objective is to use a small number of shakers to best replicate that complicated environment. Daborn experimentally demonstrated this in [14].

The acoustic loads were synthesized using a typical aerospace test specification, from SMC-016 [15]. This specification provides the shape of the auto spectrum of the pressures. This was then arbitrarily scaled to 150 dB overall sound pressure level. The correlation between all the inputs is based on the spatial correlation of a diffuse field, which allows for the input CPSD to be formed [16]. Finally, the pressure CPSD matrix was scaled by area to obtain a force CPSD matrix which is then applied to the plate FRFs to get the truth response.

Figure 13 shows the nine input locations on the plate, along with the 12 output locations. The 12 outputs are divided into two groups. Accelerometers 1, 2, 3, 5, 6, 7, 8, 10, 11, and 12 are in the "target" set, which means those ten gages are used in the force estimation process. Accelerometers 4 and 9 are in the "reference" set, which means they are not used in the force estimation process. The responses from the replica test can then be compared at gages which are used in the estimation and gages which are not. This gives some indication as to how well the overall response of the structure is captured in a given replica test.

The nine inputs are from the "good" set of input locations, which should help reduce numerical errors in the force estimation process. In addition to a good set of input locations, regularization was applied to the FRF matrices to reduce numerical error, implemented with a singular value perturbation method and a condition number threshold of 1000. Note that these input locations were selected to have a low condition number of the FRF matrix, and were not selected to optimally replicate the truth environment or provide minimum inputs.

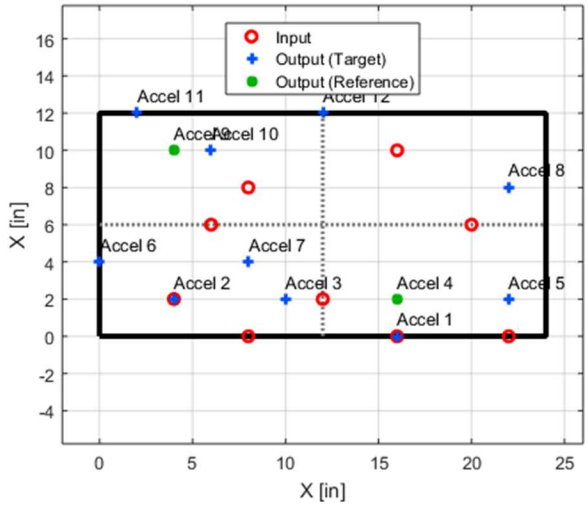

Figure 13: Plate with input and output locations

6.2 Standard Method

The first method considered is just the standard, direct force estimation method which is shown in Equation 5. In this method, the truth response CPSD for the ten gages is used as the target data and the inputs are estimated using a Moore-Penrose pseudo-inverse of the regularized FRF matrix. This solution provides the set of inputs which provide the least squares fit to the response data, in terms of not only level (APSD), but also coherence and phase since the entire CPSD response matrix is the target data.

6.3 Uncorrelated Inputs (Independent Drives)

The second method is Independent Drives, a method explored by Smallwood [8]. The inputs are assumed to be uncorrelated (independent), which requires a different form of the force estimation equation which uses the APSD of the target responses, $G_{aa,0}$, to estimate the APSD of the independent inputs, $G_{ff,1}$:

$$G_{ff,1} = (HH^*)G_{aa,0}, \tag{15}$$

where HH^* is a 10 x 9 real-valued matrix because H^* is the conjugate of the FRF matrix H. Clearly, this method makes no attempt to match the coherence or phase of the target responses.

Note that this can result in negative input APSDs, which is non-physical, so any negative values are set to zero. Also, as described by Smallwood, the inputs can be adjusted to better match the target response APSD with a simple scaling of the target responses based on the estimated responses and doing a second force estimation.

6.4 Modified Cross-Terms (Buzz Test)

The third method has been used by Daborn in recent years in a variety of multi-shaker tests [9]. This method, dubbed the buzz test method, replaces the cross terms in the target response CPSD matrix from the truth test with the coherence and phase from the system in the lab. These coherences and phases are obtained with a buzz test, wherein the shakers are attached to the structure in the lab and then uncorrelated, white noise inputs are used to excite the structure. This provides the coherence and phase of the target responses. Then, the new target response CPSD matrix can be formed using the APSDs from the truth test and the coherence and phase from the buzz test. Inputs are then estimated using the standard force estimation method.

6.5 Results

Figure 14 compares the three force estimation methods in terms of the sum of all 12 response APSDs and the sum of all nine input APSDs. Overall, the response is matched quite well by the standard and buzz test methods. Independent drives captures some of the response features, but has a fair amount of error at peaks and between peaks. The standard method has some error, primarily between peaks. The buzz test method seems to work the best to match the overall response.

The required inputs are quite different, with the standard method requiring much more force than the other two methods. Independent drives requires the least input, with the buzz test method being only slightly higher at some frequencies. As the

standard method is the only one which tries to achieve the truth test cross terms in the response, it may be assumed that matching the cross terms requires considerable force.

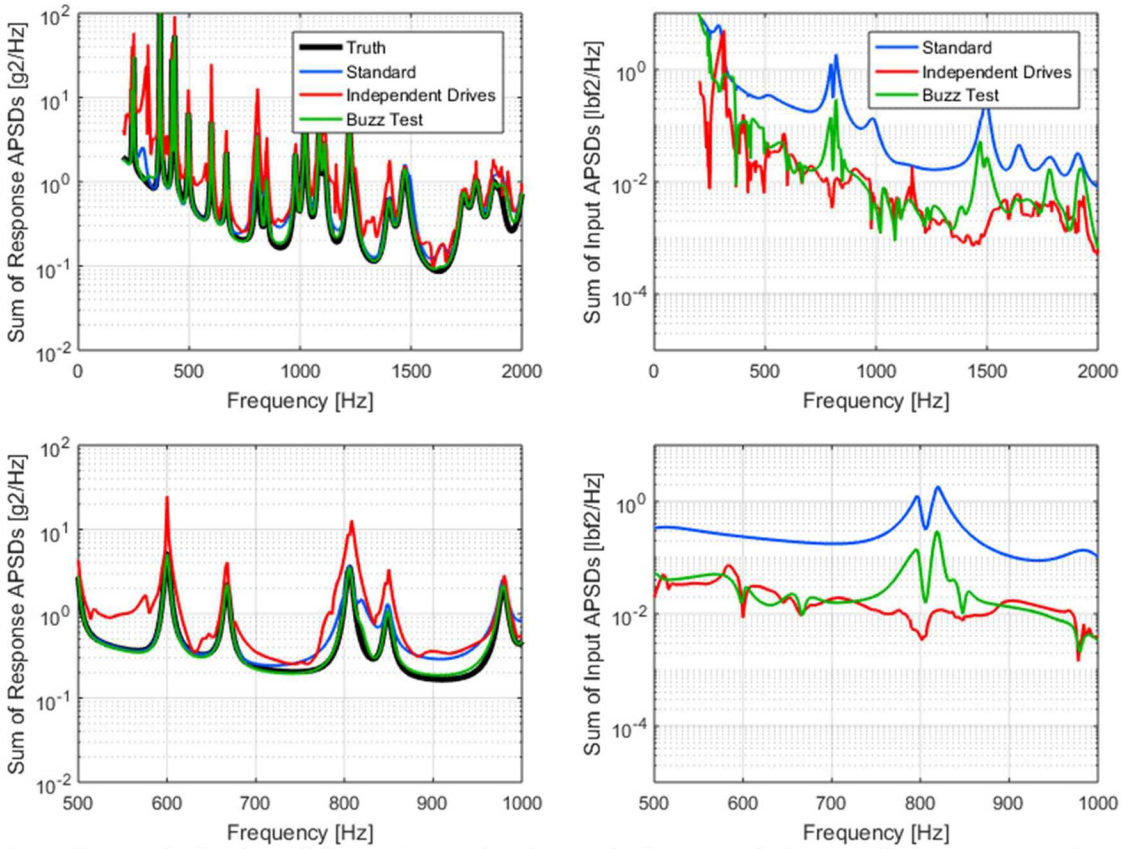

Figure 14: Replica results for three different force estimation methods. Top Left: Sum of all 12 response APSDs. Top Right: Sum of all 9 input APSDs. Bottom Left: Sum of all 12 response APSDs, zoomed to 500-1000 Hz. Bottom Right: Sum of all 9 input APSDs, zoomed to 500-1000 Hz.

Figure 15 and Figure 16 show the results in more detail, with a comparison of the APSDs at one target gage (Accel. 3) and one reference gage (Accel. 4), as well as the coherence and phase between those gages. As expected, the match to the truth response is better at the target gage than at the reference gage. Surprisingly, the standard method has quite a lot of error at the reference gage. The buzz test method and even the independent drives method do better to match the response at the reference gage. Only the independent drives method has a poor match at the target gage. Coherence and phase are notoriously difficult to assess for even simple systems. Here, it can be seen that the coherence is not well matched for the independent drives and buzz test methods, and is only approximately matched with the standard method. Phase is not captured well by any of the methods.

The results are aggregated in terms of RMS input and RMS response over the entire 200-2000 Hz band in Table 1 and

Table 2. The buzz test method has the best match to the RMS response over both target and reference gages. The independent drives method tends to over-test. The standard method is close at the target gages, but has large errors at the reference gages. In terms of inputs, the standard method requires the most input force and the independent drives method requires the least. The buzz test method is between the two for most input locations.

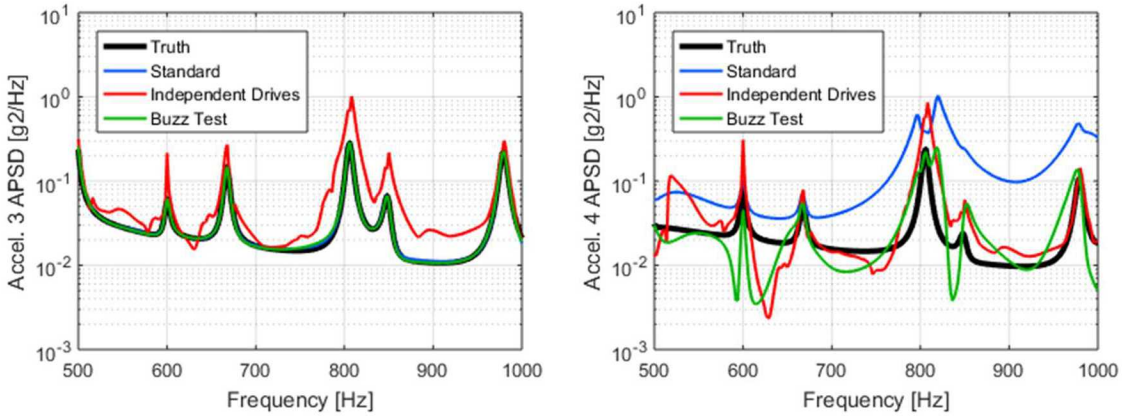

Figure 15: Response APSD at a single gage. Left: Accel. 3, in the Target gage set. Right: Accel. 4, in the Reference gage set.

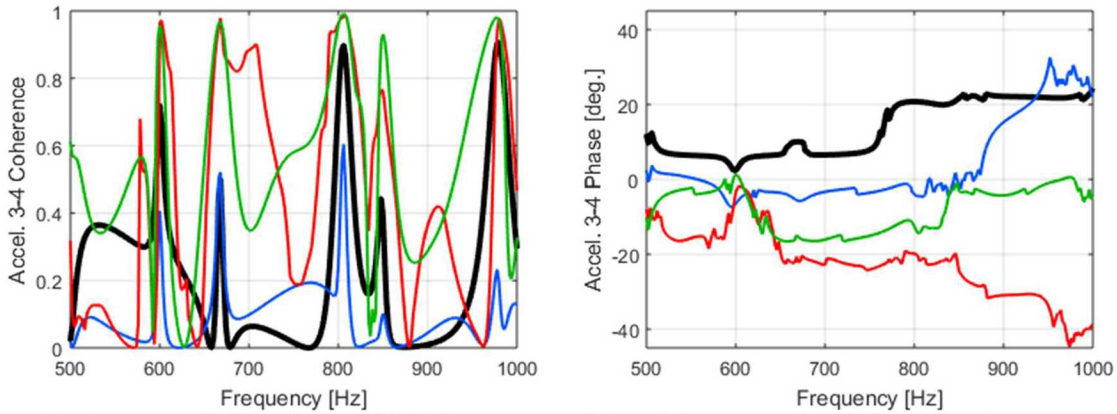

Figure 16: Coherence (left) and phase (right) between accel. 3 and 4, compared with the truth coherence and phase

Table 1: RMS response over the 200 to 2000 Hz bandwidth. Reference gages highlighted in gray.

g-RMS	Truth	Standard	Ind. Drives	Buzz Test
Output 1	19.1	19.1	29.0	19.1
Output 2	9.6	9.6	12.5	9.5
Output 3	8.7	9.2	13.9	8.9
Output 4	9.0	17.2	14.9	11.4
Output 5	9.2	9.1	14.3	9.2
Output 6	17.3	17.1	26.9	17.3
Output 7	10.5	10.2	14.4	10.2
Output 8	10.9	10.6	13.3	10.8
Output 9	9.2	10.3	11.9	8.5
Output 10	9.7	9.4	13.9	9.7
Output 11	22.4	22.2	32.1	22.4
Output 12	17.6	17.6	28.1	17.6

Table 2: RMS input over the 200 to 2000 Hz bandwidth

lbf-RMS	Standard	Ind. Drives	Buzz Test
Input 1	5.3	2.3	6.1
Input 2	5.6	3.4	4.5
Input 3	5.9	2.4	3.4
Input 4	8.6	2.9	6.5
Input 5	10.8	3.8	8.6
Input 6	16.8	3.4	8.9
Input 7	11.9	7.6	6.3
Input 8	9.2	3.5	6.5
Input 9	11.0	4.9	6.7

Singular value regularization was used to reduce the numerical error in these force estimation calculations, with a nominal condition number threshold of 1,000. As previously discussed, the amount of regularization can have an effect on the regularized FRF matrix form and the amount of error in the estimated inputs. It was observed here that the amount of regularization affected the required input forces, as shown in
Table 3 which shows the RMS input forces using condition number thresholds of 50, 100, 1000 and 10000. A condition number threshold of 10000 is nearly un-regularized and has significant errors in the inputs. These results indicate that increasing the amount of regularization can reduce the amount of input force required. A more detailed study would be needed to make general statements regarding the tradeoff between regularization, resulting input forces and response accuracy.

Table 3: RMS input using the standard force estimation method with different amounts of regularization applied, specified by the condition number threshold

lbf-RMS	C.N. 50	C.N. 100	C.N. 1,000	C.N. 10,000
Input 1	4.3	4.8	5.3	5.3
Input 2	3.7	4.5	5.6	6.1
Input 3	5.0	5.5	5.9	6.0
Input 4	6.7	7.5	8.6	8.8
Input 5	9.4	10.1	10.8	10.9
Input 6	12.5	15.0	16.8	17.0
Input 7	9.9	11.0	11.9	12.0
Input 8	7.1	8.3	9.2	9.3
Input 9	7.2	8.4	11.0	12.2

7 Conclusions

Regularization and force estimation methods were demonstrated and compared using a simple multiple-input/multiple-output dynamic system, a plate with several shakers applied. The condition number of the FRF matrix provides a measure of the matrix and its invertibility. A poorly-conditioned matrix has a high condition number, which indicates that its vectors are non-independent. This was demonstrated by contriving two systems with very different and very similar input locations. The system with the different input locations has an FRF matrix with independent vectors and the condition number was much lower than the system with very similar input locations. It was shown that changing the damping of the system does reduce the condition number because the peaks in the FRF are reduced. Random noise on each FRF in the matrix does not increase the condition number, however coherent noise (i.e. 60 Hz noise from a ground loop problem) would likely have a detrimental effect.

Regularization of the FRF matrix reduces the errors associated with performing the pseudo-inverse of a poorly-conditioned matrix. For this system, these errors were large for condition numbers greater than 1000. Both singular value and Tikhonov regularization methods proved effective at reducing errors. The amount of regularization is important; too little and the errors will not be reduced while too much will change the form of the FRF matrix, creating different errors.

Three force estimation methods were applied to determine nine shaker forces to replicate the response of the plate subject to an acoustic truth environment. None of the three methods was perfect, which is expected since the truth test here had forces at all locations on the plate and the replica test only has nine inputs. However, the standard and buzz test methods were the most effective at matching the overall response APSD. The independent drives method was less accurate for the response, but required the lowest force. The buzz test method, which replaces the truth response cross terms with new cross terms, had the best balance of response accuracy and low input forces in this case. Interestingly, while the replica response was accurate at the gages in the target set, there was some error at other, reference locations. Additionally, no method was effective at matching coherence or phase at the single gage pair of interest.

Overall, some comments can be made regarding MIMO testing and force estimation. First, regularization of the FRF matrix is likely necessary and useful to reduce numerical errors in the force estimation process, which can provide benefits to the accuracy of the replica responses and provide lower input forces. Second, each force estimation method has benefits and issues – there is a tradeoff between things like efficiency and accuracy. Pre-test predictions and modeling can be very useful to study the effects of these tradeoffs. Additionally, it was shown that simply comparing the APSDs at the control (target) locations is not a sufficient metric for assessing the response of the whole structure as the response at other locations can be inaccurate and the coherence and phase can be quite different even if the APSDs match very well. More work is needed to understand the objectives of multiple-input/multiple-output tests – should the focus be only on response levels at a small number of points, or should specifications and test objectives move toward a more full-field perspective, including more locations as well as metrics like phase, to better match not only the response acceleration but things like stress and strain as well.

References

[1] P. M. Daborn and e. al, "Next-generation random vibration tests," in *IMAC XXXII, the 32nd International Modal Analysis Conference*, Orlando, FL, 2014.

[2] R. L. Mayes and D. P. Rohe, "Physical Vibration Simulation of an Acoustic Environment with Six Shakers on an Industrial Structure," Sandia National Laboratories, 2015.

[3] R. Bernhard, "The characterization of vibration sources and measuremnt of forces using multiple operating conditions and matrix decomposition methods," in *Proceedings of Inter-Noise 2000, the 29th International Congress on Noise Control Engineering*, Nice, France, 2000.

[4] J. O'Callahan and F. Piergentili, "Force Estimation Using Operational Data," in *Proceedings of IMAC XIV, the 14th International Modal Analysis Conference*, 1996.

[5] C. R. Vogel, Computational methods for inverse problems, SIAM, the Society for Industiral and Applied Mathematics, 2002.

[6] A. E. Yagle, "Application Note: Regularized Matrix Computations, Department of EECS, the University of Michigan," [Online]. Available: http://web.eecs.umich.edu/~aey/recent/regular.pdf. [Accessed 2017].

[7] H. G. Choi, A. N. Thite and D. J. Thompson, "Comparison of methods for parameter selection in Tikhonov regularization with applicate to inverse force determination," *Journal of Sound and Vibration,* vol. 304, pp. 894-917, 2007.

[8] D. O. Smallwood, "A revised algorithm for minimum input trace to a multiple-input/multiple-output system (MIMO) to match the output autospectral densities," Sandia National Laboratories.

[9] P. M. Daborn, "Smarter Dynamic Testing of Critical Structures," PhD Thesis, University of Bristol, 2014.

[10] D. C. Kammer, "Sensor placement for on-orbit modal identification and correlation of large space structures," *Journal of Guidance, Control, and Dynamics,* vol. 14, no. 2, pp. 251-259, 1991.

[11] T. G. Carne and C. R. Dohrmann, "A modal test design strategy for model correlation," in *Proceedings of IMAC XII, the International Modal Analysis Conference*, 1994.

[12] A. N. Thite and D. J. Thompson, "Selection of resposne measurement locations to improve inverse force determination," *Applied Acoustics,* vol. 67, pp. 797-818, 2006.

[13] P. C. Hansen, Discrete inverse problems: Insight and Algorithms, SIAM: the Society for Industrial and Applied Mathematics, 2010.

[14] P. M. Daborn, "Scaling up of the Impedance-Matched Multi-Axis Test (IMMAT) Technique," in *IMAC XXXV, the 35th International Modal Analysis Conference*, Garden Grove, CA, 2017.

[15] "Test Requirements for Launch, Upper-stage and Space Vehicles, SMC Standard SMC-S-016," Air Force Space Command, Space and Missile Systems Center Standard, 2014.

[16] A. M. Smith, R. B. Davis, B. T. LaVerde, C. W. Fulcher, D. C. Jones, R. A. Hunt and J. L. Band, "Calculation of Coupled Vibroacoustics Response Estimates from a Library of Available Uncoupled Transfer Function Sets," in *Proceedings of the 53rd AIAA Structures, Structural Dynamics and Materials Conference*, Honolulu, HI, 2012.